

# Software for convenient correction of artifacts in sonomicrometry

Alexander W. Chen<sup>1</sup>, Walter Herzog<sup>1\*</sup>

<sup>1</sup>Human Performance Laboratory, University of Calgary, Alberta, Canada

\*Author for correspondence (wherzog@ucalgary.ca)

Keywords: sonomicrometry, artifacts, software

Summary statement: The occurrence and correction of artifacts in sonomicrometry is commonplace, but correction is painstaking, inconsistent, and largely undocumented. We have developed software to specifically address these issues.

## Abstract

Sonomicrometry is widely applied in biomechanics and physiology to measure precise distances with high temporal resolution. Although commonly used, its usefulness is often limited by the presence of artifacts that require correction. Unfortunately, procedures reported in the literature for artifact correction are often unclear. Furthermore, currently available tools for artifact correction require significant manual manipulations, the consistency of which takes painstaking effort to verify. To improve the efficiency and consistency of sonomicrometry, we have developed a new software tool for the correction of sonomicrometry artifacts. This tool provides a framework for artifact correction requiring fewer and more limited manipulations from the user. We aimed to make this tool more transparent and easier to use than commercially available tools. To facilitate its application, we describe the relevant properties of sonomicrometry artifacts and detail the software's correction algorithm. The software is available for MacOS and Linux with source code and documentation.

## 1 Introduction

Sonomicrometry is a technique for measuring precise distances with high temporal resolution (Rushmer et al., 1956). The distances are measured by the transmission and timing of ultrasound pulses between piezoelectric crystals. Sonomicrometry has been commonly applied to biomechanics (Azizi and Roberts, 2010; Butterfield and Herzog,

2005; Griffiths, 1987; Marsh et al., 1992; Symons et al., 2002; Tobalske et al., 2003) and to various physiological disciplines, including cardiovascular (Dione et al., 1997; Fawzy et al., 2011) and gastrointestinal physiology (Adelson et al., 2004; Armstrong et al., 2006).

Distance traces obtained from sonomicrometry are prone to artifacts that impede further analysis (Adelson and Million, 2004; Ellerby and Askew, 2007; Dione et al., 1997). Fortunately, when using digital sonomicrometry systems, these artifacts are usually easy enough to distinguish from actual data that they can be identified and rectified using heuristics. Indeed, the digital sonomicrometry systems manufactured by Sonometrics (Sonometrics Corporation, London, Canada) are packaged with software (SonoSoft) for the correction of such artifacts, and users of this system have developed or used custom software for the same purpose. (Adelson et al., 2004; Dione et al., 1997; Ellerby and Askew, 2007).

It is not uncommon, however, to obtain distance traces of poor quality such that the correction of artifacts is non-trivial. In these cases, correction is complicated by the need to judge whether or not the artifacts are correctable and just how they should be corrected. Hinging on our decision are the expenditure of time and labour (if we are overly careful), but also, more crucially, the integrity of the data (if we are not careful).

So, how best should we decide what corrections to make and how to make them? The answer to this question is unclear from the literature. Criteria for the inclusion and exclusion of data, as well as procedures for correcting artifacts, are not reported in detail. This includes the procedures used by programs designed for artifact correction, as the source codes are not publicly available.

Furthermore, poor quality distance traces typically require manual user input to address the artifacts that are mishandled by automated procedures. This can make artifact correction time-consuming and painstaking, especially for applications generating large volumes of sonomicrometry data, for instance, by the use of many crystals (Dione et al., 1997) or long recording times (Adelson and Million, 2004).

Ideally, there should be a procedure that one could apply uniformly to data in order to characterize and address artifacts in a manner justified by knowledge of the underlying sources of error, alongside a tool that automates as much of that procedure as possible.

Though we attempted to reach this ideal, we cannot claim to have attained it. However, we suggest that what we have produced represents a step towards this ideal goal.

Here, we introduce a software tool (SonoCleaner) and accompanying guidelines for the correction of sonomicrometry artifacts. Our main aim was to document at least one procedure for the correction of sonomicrometry artifacts. Furthermore, we find that the software tool is more autonomous and generally easier to use compared to SonoSoft.

In this paper, we describe the software tool from a user's perspective, the nature of sonomicrometry artifacts, and the key procedure implemented by the software tool. Separately, we discuss guidelines for the correction of sonomicrometry artifacts in the documentation of the software tool.

## **2 Materials and Methods**

### **2.1 SonoCleaner**

#### **2.1.1 Overall aims and structure of the software tool**

SonoCleaner is an open source, Creative Commons licensed software tool for the (1) efficient and (2) controlled correction of sonomicrometry artifacts.

Because sonomicrometry can generate large volumes of data that can be tedious to correct manually, we aim to handle sonomicrometry artifacts efficiently and, as much as possible, automatically. While the majority of sonomicrometry artifacts are easy to detect and correct, there are usually some artifacts for which correction is more subtle, or even ambiguous, and thus ill-advised. Thus, artifact correction in general requires judgment and precise control; we aim to provide the latter in order to empower the former.

Accordingly, the software tool is comprised of two complementary parts: (1) an automated procedure for the efficient removal of easy, unambiguous artifacts, and (2) several tools to manually address the difficult or ambiguous artifacts.

The automated procedure is not expected to correct all traces completely; it will inevitably encounter artifacts that it handles erroneously. In these cases, the user is expected to step in to remove the stumbling block (either by performing the correction manually, or deciding to reject the trace) so that the procedure can continue. This

collaboration between the user and the automated procedure is enabled by the ability to apply (and reverse) the automated procedure in fine-grained, progressive steps. In this way, the user has control over the correction of artifacts, but also the responsibility for the validity of the corrections.

### **2.1.2 Description of the user interface and features of the software tool**

Users interact with the tool through a graphical user interface. The interface displays the sonomicrometry distance trace being “cleaned” and highlights the artifacts automatically. Using the mouse, the user can zoom in and inspect portions of a trace, and can select artifacts either individually or in groups for manual correction. Manual operations are selected from a small number of preset procedures for efficiency and reproducibility. The automated procedure can be applied at any time, and can be restricted to a selected time interval.

The tool allows for the superposition of other traces on the trace under consideration in order to (a) compare them for internal consistency, and (b) to facilitate the standard practice of comparing the raw and corrected traces to ensure that corrections do not introduce new errors.

For convenience, the tool also includes functionality for (1) cropping traces, in order to focus on or export only a portion of a trace, and (2) the annotation of trace qualities, which are simply collected into a comma-separated-value (csv) file that is exported in addition to the file of the distance traces.

A demonstration of the tool on physiological data can be found in the Results (Section 3).

### **2.1.3 Where can the software tool be obtained?**

The source code and binary executables for MacOS and Linux can be downloaded from <https://github.com/awjchen/SonoCleaner/releases>. The executables are bundled with documentation that describes the features of the software tool and explains how they should be used.

### **2.1.4 Software tool limitations and future plans**

Windows operating systems are not currently supported.

Sonometrics .ssa files are currently the only format in which distance traces can be imported into or exported from the software tool. Consequently, the outputs generated by this software tool cannot be fed back into Sonometrics' SonoSoft, since, to our knowledge, SonoSoft cannot read .ssa files.

This tool requires traces with sufficiently high sampling rates in order to reliably identify artifacts and estimate slopes. In general, recordings of movements that are faster and more abrupt will require higher sampling rates.

This tool may not be suitable for precise kinematics because (1) it uses a linear interpolation procedure, and (2) it causes the uncertainties and errors in the correction of artifacts to manifest as small but abrupt changes in the distance trace.

We plan to update the software tool to try to address shortcomings as they become clear. In its current state, the software tool has room for improvement, so we would love to hear your feedback and suggestions at <https://github.com/awjchen/SonoCleaner/issues>

## **2.2 Descriptions of level-shifts and other sonomicrometry artifacts**

In order to give a description of the automated procedure, we must first touch upon the nature of sonomicrometry artifacts. Note that the following details may apply only to the sonomicrometers manufactured by Sonometrics, as data acquired with these devices were used to develop the artifact removal procedures. Moreover, we stress that the following is merely our own explanation of sonomicrometry artifacts based on empirical observations using the sonomicrometer's built-in support for viewing raw ultrasound signals with an oscilloscope.

### **2.2.1 The basic principle of sonomicrometry**

Sonomicrometry measures the time it takes for ultrasound pulses to travel between piezoelectric crystals through a medium. Given a known, constant speed of sound through the medium, a distance can be recovered.

Electrical excitation of a piezoelectric crystal produces ultrasonic vibrations that propagate outwards and can be detected at another crystal. A typical signal observed by the receiving crystal (Fig. 1A) is as follows: in chronological order, there is a excitation artifact (a consequence of the electronics), followed by a period of silence (as the

ultrasound pulse propagates), followed by an oscillation of increasing intensity (when the ultrasound pulse arrives). The arrival time of the ultrasound pulse (Fig. 1B) is defined to be the earliest time at which the intensity of the signal meets a user-defined threshold (Fig. 2, top).

(In reality, while such thresholds were used in older sonomicrometers to determine arrival times, the Sonometrics sonomicrometers use a more sophisticated triggering protocol (Vesely and Smith, 1998). However, since these thresholds are sufficient to explain the basic sonomicrometry principles we require, we will continue to use them for their simplicity.)

### **2.2.2 Mechanism and correction of “level-shift” artifacts**

However, since the magnitude of the ultrasonic vibrations can change over a recording period, due to changes in crystal orientation for instance, it is possible to obtain one of several arrival times: the threshold may be met by the first, smallest “ridge” of the oscillation; if not, it may be met by the second, slightly larger ridge; if not, perhaps the third; and so on. Thus, the arrival times may be delayed by a multiple of the oscillation period of the piezoelectric crystals. A recording that always “tracks” the same ridge produces a distance trace that is smooth and continuous. But when there is a shift in the “tracking” of the ultrasound pulse from one ridge to another, the result is a jump discontinuity in the trace, where the measured distances are suddenly displaced by some constant distance but otherwise continue to accurately mirror changes in the distance signal (Fig. 2, bottom).

These discontinuity artifacts have been termed “level-shifts”, and are the only type of artifact addressed by the automated procedure. The idea is that, because a level-shift only introduces a constant displacement to the trace, the true distances can be recovered simply by shifting back the affected portion of the trace in order to recover a smooth, continuous trace. We use the term “level-shift” to refer to the discontinuities, and not the displaced portions of the trace they cause.

### **2.2.3 Complications to the correction of level-shift artifacts**

However, there are several caveats to the simple correction of level-shifts we have just described.

(Caveat 1) In the presence of random noise, the displacement by which a level-shift should be corrected has some uncertainty. Therefore, every correction of a level-shift may introduce some error.

(Caveat 2) Data displaced by level-shifts may not precisely mirror the original. One reason for this is that there is a range of times at which a ridge could meet the detection threshold.

(Caveat 3) There are other discontinuity artifacts distinct from level-shifts in the sense that the data following these discontinuities are completely unrelated to the “true” data. This produces nonsensical data, which we view as a gap in the recording that contains no distance information. Suitably, these artifacts have been termed “dropouts”. The discontinuities associated with dropout artifacts must be distinguished from level-shifts, because correcting dropouts as if they were level-shifts introduces nonsense into the trace.

## **2.3 Methods of the automated procedure used to correct level-shifts in the software tool**

### **2.3.1 Assumptions and scope of the automated procedure**

The automated procedure proceeds under the assumption that the only artifacts in the distance trace are discontinuities produced by level-shifts; that is, we assume that the trace is broken into segments by level-shifts, where each segment is associated with a constant distance by which it has been (uniformly) displaced from its “true” value. To address random noise (Caveat 1) and, at least partially, the inexactness of level-shifts (Caveat 2), we require a tolerance level to be defined (in mm) by the user. Nonsensical artifacts (Caveat 3), and other artifacts (see the software’s documentation), are not accounted for by the automated procedure; the user must identify them and remove them manually, or must otherwise verify that they have not adversely affected the procedure.

The distance trace data are assumed to be a time series, that is, a sequence of distances spaced evenly in time. From this time series we may form the series of differences: the slopes of the lines joining the points of the original series.

The automated procedure requires as input a list of level-shifts describing the times at which the level-shifts occurred and their associated displacements. In the software tool, this list is produced by a separate level-shift labeling procedure. Like previous methods (Dione et al. 1997), the level-shifts are “detected by the first and second order derivatives”. More details on the labeling procedure may be found in the software’s documentation.

### 2.3.2 The main method used to mitigate errors while correcting level-shifts

The main idea of the automated procedure is that there are only a finite number of “levels” to which level-shifts may shift (in reasonable data, at least). Thus, a sequence of level-shifts will eventually return to a previously visited level. Under the aforementioned assumptions, this occurs exactly when the displacements of the level-shifts sum to zero, or, more practically, when they sum to within the user-specified tolerance of zero. The automated procedure searches for and acts on such groups of level-shifts, which we will call “zero-sum groups”. The process of correcting “zero-sum groups” is illustrated in Figure 3, in which the representation of level-shifts has been simplified so that their displacements match exactly with one another, without error.

But why bother to search for these groups of level-shifts? Why not simply handle each level-shift individually, for example, by recovering its slope from interpolation of the surrounding trace? Because the correction of each level-shift introduces some error that affects the relative positioning of the halves of the trace that lie before and after the level-shift; as a result, traces with more noise or many level-shifts will likely drift over time, in a random walk, from the accumulation of these small errors.

So, instead of completely eliminating the displacements of a zero-sum group of level-shifts, we merely “redistribute” the displacements by transferring all of them to the first level-shift. To illustrate this procedure, imagine that we have a zero-sum group containing exactly two level-shifts. Let the first level-shift occur earlier than the second and have an (upward) displacement  $d_1 = +1.05$  mm, and let the second level-shift have a (downward) displacement of  $d_2 = -1.00$  mm. The displacements of the level-shifts do not match exactly, since their sum is almost but not equal to zero, leaving a small error  $\epsilon = d_1 + d_2 = +0.05$  mm.



To correct this zero-sum group, we assign the level-shifts new displacements: we set the displacement of the first level-shift equal to the error ( $d'_1 = \epsilon = 0.05$  mm) and set the displacement of the second level-shift to zero ( $d'_2 = 0.00$  mm). This “redistribution” operation has the effect of taking the portion of the trace lying between the two level-shifts and then shifting it downwards to a new position such that the second level-shift is completely eliminated. Because of the error  $\epsilon$ , the new position of this intermediary region may not be precisely correct.

However, the total change in displacement brought about by this operation is zero: we have added a displacement of  $-1.00$  mm to the first level-shift, and another equal but opposite displacement of  $+1.00$  mm to the second. Therefore, the operation changes the position of only the intermediary region, and leaves the rest of the trace untouched. Thus, any inaccuracies caused by the error  $\epsilon$  are confined to this intermediary region. This approach helps to reduce the aforementioned accumulation of error.

We can apply the same procedure to handle zero-sum groups containing more than two level-shifts. Let a zero-sum group contain  $n$  level-shifts with displacements  $d_1, d_2, \dots, d_n$ . We assign the first level shift a displacement of  $d'_1 = \epsilon = d_1 + d_2 + \dots + d_n$ , while the others are assigned displacements of zero, that is,  $d'_2 = d'_3 = \dots = d'_n = 0$ . As before, since the total change in displacement caused by this operation is zero, the operation only affects the portion of the trace within the span of the level-shifts, thereby reducing the accumulation of error.

### 2.3.3 Additional aspects of level-shift correction

Of course, the “true” displacement of a level-shift might not be zero, for example, when a level-shift occurs during a period of quick movement. Therefore, we do not act on the “raw” displacement of a level-shift, but the difference of its displacement from a target slope estimated from the surrounding trace. To compute this target slope, we take several slope segments on each side of the level-shift (4 each, for 8 total), exclude other level-shifts, and take the median of the remaining slopes to be the target slope, but only if a Wilcoxon signed-rank matched-pair test (where the slopes of the segments are paired with zeros) rejects its null hypothesis at  $\alpha = 0.10$ ; otherwise the target slope is set to zero. This method is intended to be conservative so that it avoids estimating slopes in noisy data (where it may make inaccurate estimates).

Furthermore, we would like to constrain zero-sum groups to be more “natural”. Level-shifts that occur in close time-proximity, and follow after each other directly, are intuitively more likely to form a proper “match” than those that do not. Therefore, we constrain zero-sum groups of level-shifts to be contiguous subsequences of level-shifts (that is, a zero-sum group must not “skip over” any level-shifts), and stipulate that zero-sum groups spanning shorter intervals of time are considered before those that span longer intervals. Additionally, since reasonable data should only contain a finite number of “levels”, there should be a maximum number back-to-back level-shifts that do *not* form a zero-sum group; accordingly, we place an upper limit to the size of a zero-sum group (8 level-shifts).

Note, however, that we are not able to completely eliminate the uncertainty and error associated with the correction of level-shifts (Caveats 1 and 2) because the “redistribution” of displacements merely restricts the error to a smaller portion of the trace. Therefore, traces requiring more frequent and difficult corrections should generally be less accurate, and thus this artifact correction procedure should not be considered a substitute for clean, artifact-free traces obtained from superior experimental technique.

### 3 Results

We demonstrate the use of the software tool to correct small portions of two distance traces. The correction of the first trace (Fig. 4) is unambiguous and is representative of the typical process of correction using the software tool. The correction of the second trace (Fig. 5) is performed merely to showcase the capabilities of the software tool; in practice, traces as poor as the second example should probably not be corrected due to the risk of unknowingly introducing errors.

#### 3.1 Demonstration of the software tool on a typical artifact-laden trace

The first trace (Fig. 4) records distances between two crystals embedded in the medial gastrocnemius muscle of a rabbit. The trace records the active contraction of the medial gastrocnemius (induced by electrical stimulation). Figure 4A shows the raw trace (as seen through the software tool’s user interface) with level-shifts highlighted in alternating yellow and magenta. While there are many level-shifts, the correction of this

trace is unambiguous: we can see that the trace merely switches back and forth between two “levels”.

We begin correction with the application of the automatic procedure, which handles all but two level-shifts (Fig. 4B). The modified segments of the trace have been highlighted in alternating white and cyan. To complete the corrections, we manually translate the portion of the trace between the two remaining level-shifts according to our judgment (Fig. 4C). This operation leaves the first level-shift with significant residual error. It is this large error that prevented the automated procedure from processing the last two level-shifts. (In this case, we have opted to perform the correction ourselves, judging this error to be tolerable for our purposes.) We then compare our corrections to the uncorrected version of the trace, superimposed in magenta, and to the artifact-free “twin trace” (the distance trace obtained by swapping the transmitting and receiving roles of the crystal pair), superimposed in green (Fig. 4C). Our corrections are shown to be consistent with the twin trace.

### **3.2 Demonstration of the software tool on a very low quality trace**

The second trace (Fig. 5) is taken from a dry-run experiment in which crystals were embedded into a false vertebral artery (tubing filled with ultrasound gel), which was stretched in response to chiropractic manipulation of a model head and neck. We selected a portion of the worst salvageable trace so that the raw trace (Fig. 5A) is riddled with artifacts. The worst portions of the distance trace traverse six different “levels” and have level-shifts between almost every data point.

Due to the unusually poor quality of this trace, we begin by adjusting the level-shift labeling parameters (not shown). We then apply the automated procedure, which leaves three level-shifts (Fig. 5B). These three level-shifts are corrected manually by setting their displacements to estimates of the slope of the surrounding trace (Fig. 5C). Finally, we compare our corrections to the uncorrected version of the trace, superimposed in magenta (also Fig. 5C).

While the corrected trace is compatible with the other (artifact-free) traces from its recording, we cannot directly verify the accuracy of our corrections due to the absence of signal on the twin trace. In this case, it is not feasible to guarantee that no errors were introduced in the correction of this poor quality trace.

## 4 Concluding remarks

Processing of sonomicrometry data often requires the correction of artifacts, but the procedures for such corrections are not reported in detail in the literature. To address this issue, we developed, and made publicly available, a software tool and guidelines for performing such corrections. We hope that the materials we have provided will help to improve the reproducibility of sonomicrometry data processing by providing a point of reference.

## 5 Acknowledgments

Thanks to T. R. Leonard, B. R. MacIntosh, S. Sibole, and I. C. Smith for their critical reading of the manuscript, to L. Gorrell and C. Waters-Banker for the use of their data, and to L. Gorrell and R. Madden for their assistance in testing the software tool.

## 6 Competing interests

The authors declare no competing or financial interests.

## 7 Funding

This work was supported by grants from NSERC of Canada, The Canada Research Chair Program, and the Killam Foundation.

## 8 Data availability

Source code, executables, and documentation are available at <https://github.com/awjchen/SonoCleaner/releases>.

The raw sonomicrometry data files and artifact-labeling parameters used to generate Figures 4 and 5 are included in the Supplementary Information.

## 9 References

1. **Adelson, D. W., & Million, M.** (2004). Tracking the moveable feast: sonomicrometry and gastrointestinal motility. *Physiology*, **19(1)**, 27–32.
2. **Adelson, D. W., Million, M., Kanamoto, K., Palanca, T., & Taché, Y.** (2004). Coordinated gastric and sphincter motility evoked by intravenous CCK-8 as monitored by ultrasonomicrometry in rats. *American Journal of Physiology-Gastrointestinal and Liver Physiology*, **286(2)**, G321–G332.
3. **Armstrong, S. R., McCullough, J. L., & Beattie, D. T.** (2006). Measurement of 5-HT<sub>4</sub> receptor-mediated esophageal responses by digital sonomicrometry in the anesthetized rat. *Journal of Pharmacological and Toxicological Methods*, **53(3)**, 198–205.
4. **Azizi, E., & Roberts, T. J.** (2010). Muscle performance during frog jumping: influence of elasticity on muscle operating lengths. *Proceedings of the Royal Society B: Biological Sciences*, **277(1687)**, 1523–1530. <https://doi.org/10.1098/rspb.2009.2051>
5. **Butterfield, T. A., & Herzog, W.** (2005). Quantification of muscle fiber strain during in vivo repetitive stretch-shortening cycles. *Journal of Applied Physiology*, **99(2)**, 593–602.
6. **Dione, D., Shi, P., Smith, W., DeMan, P., Soares, J., Duncan, J., & Sinusas, A.** (1997). Three-dimensional regional left ventricular deformation from digital sonomicrometry. In *Engineering in Medicine and Biology Society, 1997. Proceedings of the 19th Annual International Conference of the IEEE (Vol. 2, pp. 848–851)*. IEEE. Retrieved from <http://ieeexplore.ieee.org/abstract/document/757790/>
7. **Ellerby, D. J., & Askew, G. N.** (2007). Modulation of pectoralis muscle function in budgerigars *Melopsittacus undulatus* and zebra finches *Taeniopygia guttata* in response to changing flight speed. *Journal of Experimental Biology*, **210(21)**, 3789–3797. <https://doi.org/10.1242/jeb.006296>
8. **Fawzy, H., Fukamachi, K., Mazer, C. D., Harrington, A., Latter, D., Bonneau, D., & Errett, L.** (2011). Complete mapping of the tricuspid valve apparatus using three-dimensional sonomicrometry. *The Journal of Thoracic and Cardiovascular Surgery*, **141(4)**, 1037–1043. <https://doi.org/10.1016/j.jtcvs.2010.05.039>

9. **Griffiths, R.** (1987). Ultrasound transit time gives direct measurement of muscle fibre length in vivo. *Journal of Neuroscience Methods*, **21(2)**, 159–165.
10. **Marsh, R. L.** (2016). Speed of sound in muscle for use in sonomicrometry. *Journal of Biomechanics*, **49(16)**, 4138–4141. <https://doi.org/10.1016/j.jbiomech.2016.10.024>
11. **Marsh, R. L., Olson, J. M., & Guzik, S. K.** (1992). Mechanical performance of scallop adductor muscle during swimming. *Nature*, **357(6377)**, 411.
12. **Rushmer, R. F., Franklin, D. L., & Ellis, R. M.** (1956). Left ventricular dimensions recorded by sonocardiometry. *Circulation Research*, **4(6)**, 684–688.
13. **Symons, B. P., Leonard, T., & Herzog, W.** (2002). Internal forces sustained by the vertebral artery during spinal manipulative therapy. *Journal of Manipulative and Physiological Therapeutics*, **25(8)**, 504–510.
14. **Tobalske, B., Hedrick, T., Dial, K., & Biewener, A.** (2003). Comparative power curves in bird flight. *Nature*, **421(6921)**, 363.
15. **Vesely, I., & Smith, W. L.** (1998). U.S. Patent No. 5,779,638. Washington, DC: U.S. Patent and Trademark Office.

## Figures

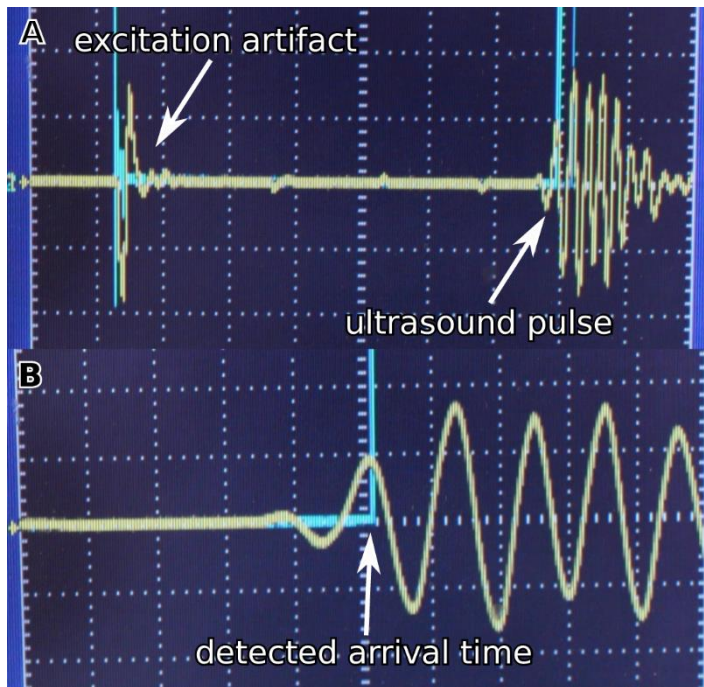


Figure 1. An ultrasound signal observed by a receiving sonomicrometry crystal, viewed using the sonomicrometer's built-in support for displaying ultrasound signals on an oscilloscope. The horizontal axis represents time, while the vertical axis represents voltage (signal strength). The ultrasound signal appears in yellow, while the signal indicating the time of arrival of the ultrasound pulse appears in blue. (A) The full ultrasound signal from the excitation of the transmitting crystal to the reception of the ultrasound pulse. (B) A closeup of the ultrasound pulse. Ultrasound pulses vary considerably in shape; this particular ultrasound pulse was selected for its susceptibility to level-shifts.

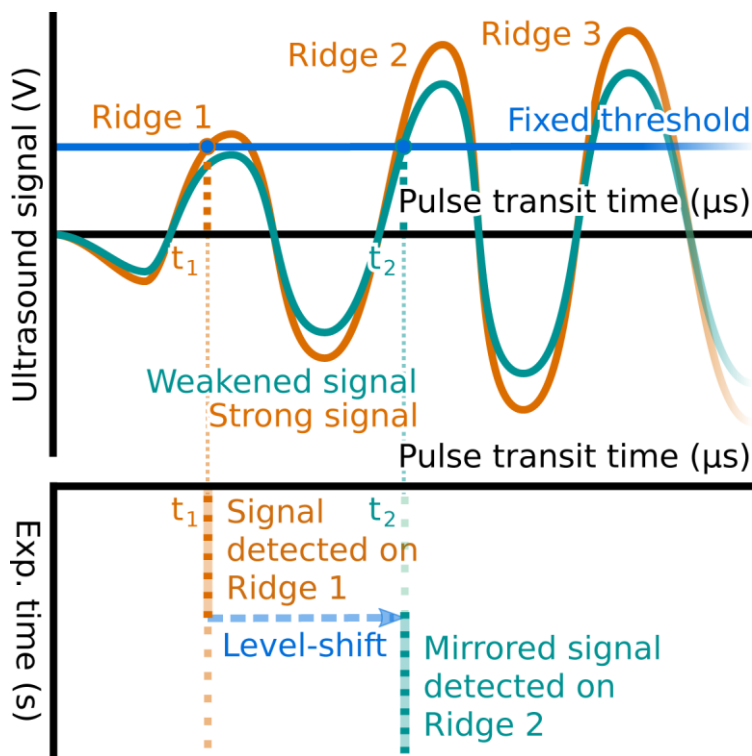


Figure 2. A simplified mechanism for level-shifts based on empirical observations using the sonomicrometer's built-in support for viewing raw ultrasound signals with an oscilloscope.

Top: An idealized close-up of two ultrasound pulses as observed by a receiving crystal; the first is shown in orange, and the second is a weakened version of the first shown in teal. The horizontal axis represents the time elapsed since the emission of the ultrasound pulse from a separate transmitting crystal (on the order of microseconds and related to the distance by the speed of sound), and the vertical axis represents the intensity of the ultrasound signal.

An ultrasound pulse is a series of oscillations (or “ridges”) of increasing intensity that is detected when its amplitude first exceeds a fixed threshold. Changes in the strength of the ultrasound signal can cause the threshold to be triggered on a different ridge, thus causing a level-shift.

Bottom: The distance trace associated with the weakening ultrasound pulse in the upper panel, but rotated 90 degrees clockwise so that it may be aligned with the upper panel. The independent variable (now on the vertical axis) represents the time elapsed during



the experiment (on the order of seconds and sampled discretely at a fixed frequency), and the dependent variable (now on the horizontal axis) represents the pulse transmit time, as in the upper panel. Each dot (i.e. each sample) of the distance trace corresponds to the emission and reception of a single ultrasound pulse.

A change in the triggering ridge manifests as a jump discontinuity where the signal following the discontinuity is a continuation of the signal prior, except with an added, fixed offset. The shifted signal following the discontinuity “mirrors” what it would have been if the strength of the ultrasound signal had remained constant.

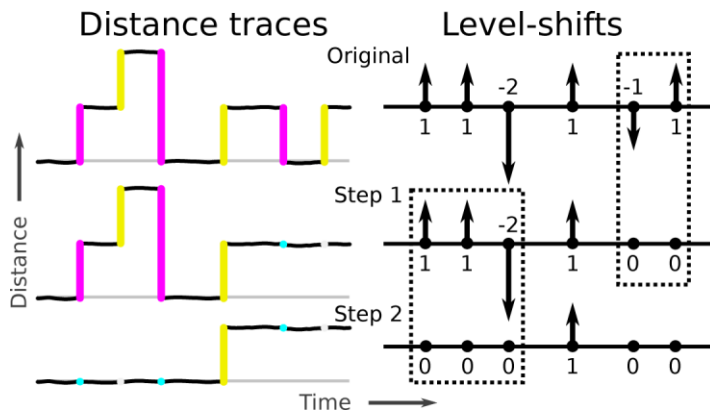


Figure 3. A simplified illustration of the action of the automated procedure on “zero-sum groups”. The left column displays idealized distance traces in the style of the software tool: the horizontal axis represents time, while the vertical axis represents distance; uncorrected level-shifts are highlighted in alternating magenta and yellow, while modified level-shifts appear in alternating cyan and white. If not for the level-shifts, the distance traces would be constant with respect to time (gray lines). The right column displays the corresponding representations of level-shifts used by the automated procedure: level-shifts are characterized by their displacement and the time of their occurrence. The displacements of the level-shifts have been simplified to be whole numbers; in particular, the displacements of the level-shifts match one another with no error. The rows represent the state of a single distance trace as it is transformed by successive steps of the automated procedure. The dashed boxes in the right column highlight the action of the automated procedure: one at a time, “zero-sum groups” (groups of level-shifts which have a total displacement of zero) are found and eliminated by “canceling-out” the level-shifts. This figure replicates the behaviour of the automated procedure in the software tool, but the simplicity of the level-shifts does not reveal certain aspects of the procedure’s behaviour, nor have we fully explained the observable behaviour. For a more complete description, see sections 2.3.2 and 2.3.3.

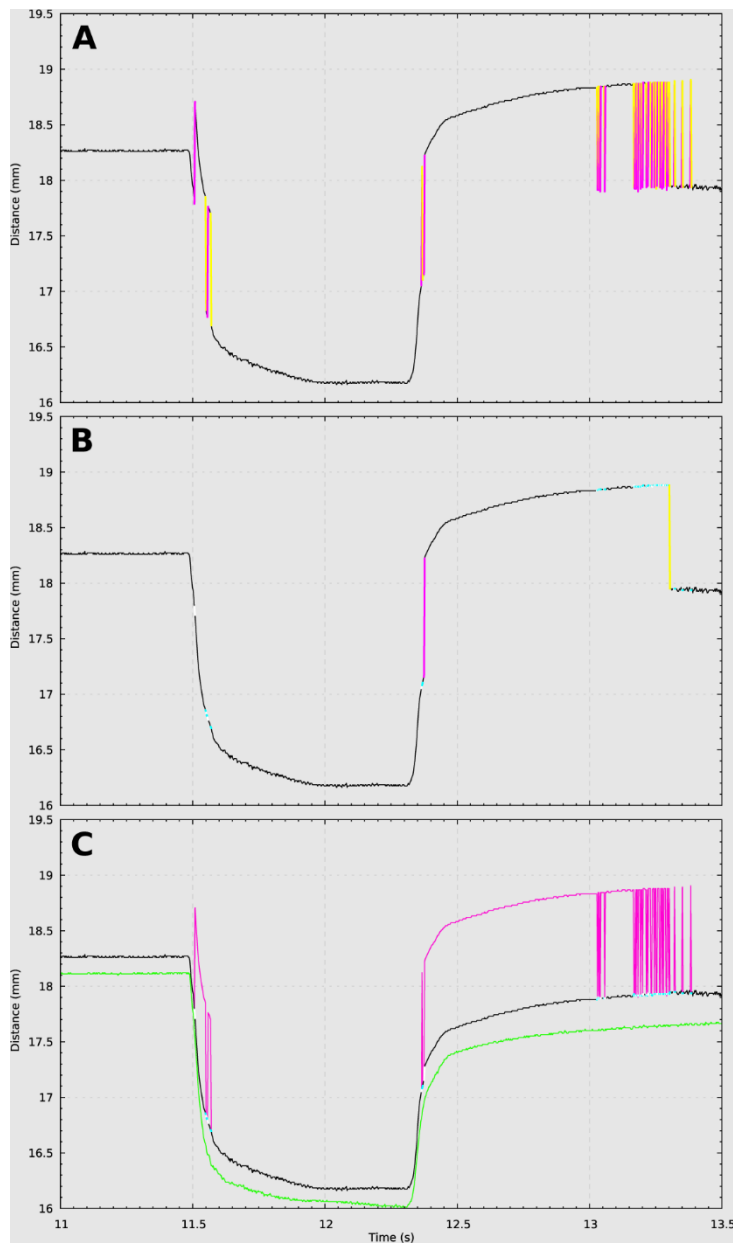


Figure 4. Removing artifacts from a typical artifact-laden trace using the software tool. (A) The original trace with highlighted artifacts in magenta and yellow. (B) Application of the automated procedure leaves two artifacts which must be corrected by hand. (C) The remaining corrections are performed manually to complete the correction. For verification, the corrected trace (black) is superimposed with, and compared to, the uncorrected trace (magenta) and the “twin trace” (green).

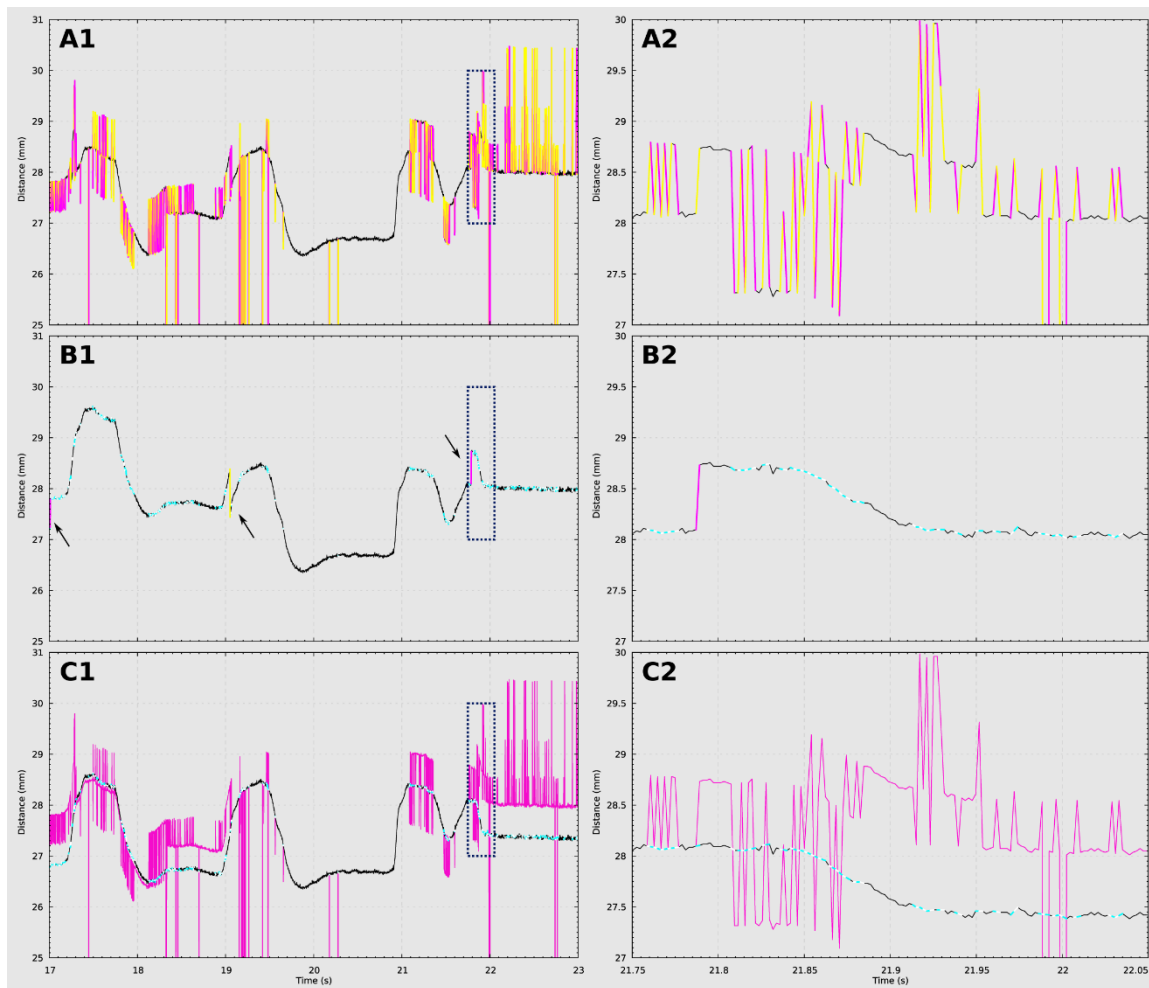


Figure 5. Removing artifacts from a selected portion of a very low quality trace. In practice, the correction of traces as poor as this one should probably not be attempted due to the risk of unknowingly introducing errors. Column 1 displays the selected portion of the trace, while Column 2 displays a closeup of the area within the dashed rectangle so that individual data points may be distinguished. (Row A) The original trace with highlighted artifacts in magenta and yellow. (Row B) Application of the automated procedure leaves three artifacts, indicated by the arrows, which must be corrected by hand. (Row C) The remaining corrections are performed manually to complete the correction. For verification, the corrected trace is compared to the uncorrected trace (superimposed in magenta); no “twin trace” was available for comparison.